

The hyperfine splitting in QCD mesonic screening masses at asymptotically large temperatures

Marco Cè^{a,b} Leonardo Giusti^{a,b} Davide Laudicina^c Michele Pepe^b Pietro Rescigno^{a,b}

^a*Department of Physics “Giuseppe Occhialini”, University of Milano-Bicocca,
Piazza della Scienza 3, I-20126 Milano, Italy*

^b*INFN Milano-Bicocca,
Piazza della Scienza 3, I-20126 Milano, Italy*

^c*Fakultät für Physik und Astronomie, Institut für Theoretische Physik II, Ruhr-Universität Bochum,
44780 Bochum, Germany*

E-mail: marco.ce@unimib.it, leonardo.giusti@unimib.it,
davide.laudicina@ruhr-uni-bochum.de, michele.pepe@mib.infn.it,
p.rescigno1@campus.unimib.it

ABSTRACT: We determine the hyperfine splitting in the QCD flavour non-singlet mesonic screening masses at asymptotically large temperatures. The analytic calculation is carried out in the dimensionally-reduced effective theory where the first non-zero contribution is of $O(g^4)$ in the QCD coupling constant g . Apart for its own theoretical interest, this result provides instrumental information to interpret and to parameterize non-perturbative data that are being produced at very high temperatures by numerical simulations of lattice QCD. Indeed, the comparison with existing non-perturbative results shows that higher order (non-perturbative) contributions in g are needed to explain the data up to the highest temperatures explored, which is of the order of the electroweak scale.

Contents

1	Introduction	1
2	Preliminaries	3
3	Effective description	4
3.1	Effective action	4
3.2	Non-relativistic fermionic action	5
3.3	Fermionic equations of motion	6
3.3.1	Perturbative expansion	6
4	Mesonic correlators	7
4.1	Free-theory limit	8
4.2	Next-to-leading order	8
4.2.1	Spin-independent contribution	9
4.2.2	Spin-dependent contribution	10
5	Hyperfine splitting	10
5.1	Leading contribution	11
5.2	Analysis of the wave-function	12
6	Comparison with non-perturbative results	13
7	Conclusions	15
A	Simplification of the fermionic action	17
B	Propagators in the free theory	17
C	Equations of motion at next-to-leading order	18
D	Evaluation of the static potential	19
D.1	Spin-independent contribution	19
D.2	Spin-dependent contribution	19

1 Introduction

The dynamics of the strong interactions at high temperature plays a key rôle in several physical processes, from the cosmological evolution of the early universe, to the interpretation of

the experimental data at the relativistic heavy ion collision facilities. Since Quantum Chromodynamics (QCD) is asymptotically free, one could hope that, for sufficiently high temperatures, its dynamics can be efficiently described perturbatively. Nevertheless, at asymptotically high temperatures, QCD effectively behaves as a three-dimensional Yang-Mills theory which exhibits confinement and, therefore, has to be solved non-perturbatively [1]. As a consequence, the perturbative series in the strong coupling constant g of a given physical quantity can only be computed up to a certain order, after which non-perturbative effects start to appear. A well-known example is the QCD Equation of State for which it is possible to compute perturbatively only terms up to $O(g^6 \ln(g))$ [2, 3]. A further issue regarding thermal perturbation theory is the observed slow convergence of the series, even at very high temperatures. As a result, the non-perturbative dynamics turns out to be relevant up to temperatures orders of magnitude larger than the GeV scale. This kind of behaviour has been observed first in the SU(3) Yang-Mills theory [4, 5], and then only very recently also in QCD [6–9].

Mesonic screening masses characterize the behaviour of spatially-separated correlation functions. They are the inverse of spatial correlation lengths, and describe the response of the quark-gluon plasma when a meson with a given set of quantum numbers is injected into the system. Flavour non-singlet mesonic screening masses at zero Matsubara frequency are among the simplest quantities that can be computed in the thermal theory, and therefore they are an ideal playground for comparing analytic results with non-perturbative data. In perturbation theory they have been calculated at the next-to-leading order in the dimensionally-reduced effective theory some time ago [10], while baryonic screening masses with nucleon quantum numbers have been computed at the same order only very recently [11]. Non-perturbatively, the steady conceptual, algorithmic and technological progress in lattice QCD has made it possible numerical computations of mesonic and baryonic screening masses in a wide range of temperature with permille accuracy [7, 8, 12].

The aim of this paper is to calculate the leading contribution of order $O(g^4)$ to the (hyperfine) splitting between the masses at zero Matsubara frequency in the pseudoscalar and in the vector channels at asymptotically large temperature. The hyperfine splitting is of particular interest in thermal QCD, as well as for quarkonia in QCD at zero temperature [13], because it is sensitive (a) to all the three scales entering the effective theory, namely the hard πT , the soft m_E and the ultrasoft g_E^2 one, and (b) to non-perturbative contributions to the potential of the relevant Schrödinger equation. The high accuracy of the lattice data that has been reached recently made it possible to clearly resolve the hyperfine splitting between the masses in the pseudoscalar and in the vector channel up to temperatures of the order of the electroweak scale [7]. All these facts make the hyperfine splitting an ideal quantity to test the effective field theory construction against non-perturbative results, and to scrutinize the range of applicability of its perturbative treatment. Finally, knowing analytically the leading $O(g^4)$ contribution is instrumental to interpret and to parameterize non-perturbative data.

This paper is organized as follows. In Section 2 we define the interpolating fields and their two-point correlation functions in QCD, as well as the concept of screening masses. Section 3 is devoted to briefly introduce the effective field theory framework in which the

calculation of the hyperfine splitting is carried out. Here we also introduce the equations of motion and the expression of the quark propagators at leading and next-to-leading orders. In Section 4 the interpolating fields already introduced in Section 2 are re-expressed in the context of the three-dimensional effective theory, and the two-dimensional Schrödinger equations satisfied by the corresponding correlation functions are derived. The computation of the hyperfine splitting is carried out in Section 5, while in Section 6 we compare our result with the non-perturbative data in Ref. [7]. Finally we discuss our conclusions in Section 7. Additional technical details are reported in four appendices.

2 Preliminaries

In this paper we focus on the flavour non-singlet pseudoscalar and vector screening masses at zero Matsubara frequency related to the interpolating fields

$$\mathcal{O}^a(x_0, x) = \bar{\psi}(x_0, x) \Gamma_{\mathcal{O}} T^a \psi(x_0, x), \quad (2.1)$$

where $\mathcal{O} = \{P, V_2\}$, $\Gamma_{\mathcal{O}} = \{\gamma_5, \gamma_2\}$, and we make the definite choice of selecting the component for the vector current in direction 2. The T^a are the $a = 1, \dots, N_f^2 - 1$ generators of the $SU(N_f)$ algebra, normalized so that $\text{Tr}[T^a T^b] = \delta^{ab}/2$, which dictate the flavour structure of the interpolating fields. The two-point screening correlation functions considered in this paper are

$$\mathcal{C}_{\mathcal{O}}(x_3) = \int_0^{1/T} dx_0 \int_{\mathbf{R}} \langle \mathcal{O}^a(x_0, x) \mathcal{O}^a(0) \rangle, \quad x = (\mathbf{R}, x_3), \quad (2.2)$$

where no summation over the flavour index a is understood. Here $\int_{\mathbf{R}} = \int d^2\mathbf{R}$ denotes the integration over the transverse spatial directions. Since we are assuming mass-degenerate quarks, the two-point correlation functions above are independent on the flavour structure of the interpolating fields, and therefore we drop the flavour index a on the l.h.s. of eq. (2.2). The corresponding screening masses probe the exponential fall-off of the screening correlators at asymptotically large distances, and are defined as

$$m_{\mathcal{O}} = - \lim_{x_3 \rightarrow \infty} \frac{d}{dx_3} \ln [\mathcal{C}_{\mathcal{O}}(x_3)]. \quad (2.3)$$

The $O(g^2)$ next-to-leading correction to $m_{\mathcal{O}}$ was computed in the three-dimensional effective theory in Refs. [10, 14]. For three massless quarks, its expression reads

$$m_{\mathcal{O}}^{\text{nlo}} = 2\pi T (1 + 0.032740 \cdot g^2), \quad (2.4)$$

where the first term on the r.h.s. is the free-field theory value, while the second one is due to interactions. Notice that, at $O(g^2)$ the value of the screening mass is independent of the field \mathcal{O}^a defined in eq. (2.1), i.e. it is spin-independent. This is because the hyperfine splitting, defined as

$$\Delta m_{\text{VP}} = m_{\text{V}} - m_{\text{P}}, \quad (2.5)$$

starts at $O(g^4)$, see below.

3 Effective description

In thermal QCD at large temperatures, gauge fields in the zero Matsubara sector are the relevant degrees of freedom at distances much larger than the extent of the compact direction. The contributions from the non-zero Matsubara sectors ($n \neq 0$) are strongly suppressed due to their heavy “masses” that are $\sim 2n\pi T$ ($n \in \mathbb{Z}$). Quark modes, due to anti-periodic boundary conditions, are always heavy with “masses” $\sim (2n + 1)\pi T$. In this context the physics that takes place at energies much lower than T , or equivalently that involves distances much larger than the compact direction, can be described by a three-dimensional effective SU(3) Yang-Mills theory [2, 15, 16].

3.1 Effective action

The effective theory contains gauge fields A_k , with $k = 1, 2, 3$, living in three spatial dimensions. They are coupled to a massive scalar field A_0 , which transforms under the adjoint representation of the gauge group. The action of the effective theory, called Electrostatic QCD (EQCD), reads [15, 16]

$$S_{\text{EQCD}} = \int d^3x \left\{ \frac{1}{2} \text{Tr} [F_{jk} F_{jk}] + \text{Tr} [(D_j A_0) (D_j A_0)] + m_{\text{E}}^2 \text{Tr} [A_0^2] \right\} + \dots, \quad (3.1)$$

where the trace is over the color index¹, and the dots stand for contributions from higher-dimensional fields [17]. Here $j, k = 1, 2, 3$ and $[D_j, D_k] = -ig_{\text{E}} F_{jk}$ with the covariant derivative defined as² $D_j = \partial_j - ig_{\text{E}} A_j$. The low-energy constants m_{E}^2 and g_{E}^2 are the Lagrangian mass squared of the scalar field A_0 and the dimensionful coupling constant of the three-dimensional Yang-Mills theory, respectively. They have been perturbatively matched to QCD in Refs. [18–20]. At leading order they read

$$m_{\text{E}}^2 = g^2 T^2 \left(\frac{N_c}{3} + \frac{N_f}{6} \right) + O(g^4 T^2), \quad g_{\text{E}}^2 = g^2 T + O(g^4 T), \quad (3.2)$$

where g is the QCD coupling constant, N_f is the number of flavours and N_c is the number of colours. Therefore, at asymptotically high temperatures, the scalar field with mass m_{E} represents a heavy mode w.r.t. the gauge field. When studying physics that takes place at energies much lower than m_{E} , the field A_0 can be integrated out, and the action of the resulting effective theory, usually called Magnetostatic QCD (MQCD), reads

$$S_{\text{MQCD}} = \frac{1}{2} \int d^3x \text{Tr} [F_{jk} F_{jk}] + \dots \quad (3.3)$$

Note that, being a three-dimensional Yang-Mills theory with coupling $g_{\text{M}} = g_{\text{E}} + \dots$, its dynamics is non-perturbative at all temperatures [1] with g_{M} that sets the scale in the theory already at the classical level.

¹Throughout the paper we use the symbol Tr to indicate the trace over the indices of the matrix, i.e. the trace can be over colour and/or spin indices. Analogously the symbol $\mathbb{1}$ is the identity in colour and/or spin indices.

²In the effective theory we adopt the usual perturbative normalization of the gauge field.

As a result, QCD develops three different energy scales namely g_E^2 , m_E , and πT which, for sufficiently high temperatures, satisfy the hierarchy

$$\frac{g_E^2}{\pi} \ll m_E \ll \pi T \quad \longrightarrow \quad \frac{g^2}{\pi^2} \ll \frac{g}{\pi} \ll 1, \quad (3.4)$$

where on the r.h.s. we used the expressions at leading order for g_E^2 and m_E in eq. (3.2).

3.2 Non-relativistic fermionic action

As anticipated, at high temperatures quarks are heavy fields and their dynamics can be effectively described by a 3-dimensional non-relativistic QCD (NRQCD) [21–23]. The lightest fermion modes are those in the Matsubara sectors $n = 0, -1$ with a “mass” of πT . By following the derivation in Appendix A of Ref. [11] supplemented by the leading spin-dependent terms, the effective action for a single flavour in the $n = 0$ Matsubara sector, which couples to soft and ultrasoft gauge fields, reads

$$S_{\text{NRQCD}} = i \int d^3x \left\{ \bar{\chi} \left[M - g_E A_0 + D_3 - \frac{1}{2\pi T} \left(D_\perp^2 + \frac{g_E}{4i} [\sigma_j, \sigma_k] F_{jk} \right) \right] \chi \right. \\ \left. + \bar{\phi} \left[M - g_E A_0 - D_3 - \frac{1}{2\pi T} \left(D_\perp^2 + \frac{g_E}{4i} [\sigma_j, \sigma_k] F_{jk} \right) \right] \phi \right\} + \dots, \quad (3.5)$$

where $j, k = 1, 2$ and χ and ϕ are three-dimensional two-component spinor fields, see Ref. [10, 11, 24]. In eq. (3.5) the fields χ and ϕ propagate forward and backward in the third spatial direction, respectively. For the clarity of the presentation we do not report the corresponding contributions for the fields in the fermionic Matsubara sector $n = -1$, with backward propagating χ fields and forward propagating ϕ fields in the third spatial direction respectively. These fields contribute to the correlators of interest for this work with the very same Wick contractions of those in the $n = 0$ sector, and we will account for their contribution in the prefactors of their expressions. In eq. (3.5) we have already made explicit the expressions of the low energy constants appearing in front of the various terms at the order we are interested, e.g. the coupling appearing in front of the spin-dependent term coincide at this order with g_E given in eq. (3.2) and appearing in the covariant derivatives. Finally, the expression of M at $O(g^2)$ reads [10]

$$M = \pi T \left(1 + \frac{g^2}{8\pi^2} C_F \right), \quad \text{where} \quad C_F = \frac{N_c^2 - 1}{2N_c}. \quad (3.6)$$

The leading contribution to the hyperfine splitting in the mesonic screening masses is due to the non-diagonal (in spinor indices) term in eq. (3.5), and it is due to the exchange of ultrasoft gluons between two quark propagators, whose dynamics is described by the Yang–Mills part of the action in eq. (3.1). In analogy with the power counting rules established in Table 1 of Ref. [11], by looking at the EQCD action and by taking into account that the relevant dimensionful scale is g_E^2 , it follows that $F_{jk} = O(g_E^3)$. As a consequence, the non-diagonal term (in spinor indices) in eq. (3.5) satisfies the power counting rule

$$g_E [\sigma_j, \sigma_k] F_{jk} = O(g_E^4), \quad (3.7)$$

which translates, by using eq. (3.2), into a term of $O(g^4)$. By taking into account the discussion reported in Appendix A, the non-relativistic effective action in eq. (3.5) can be written in a compact way as

$$S_{\text{NRQCD}} = i \int d^3x [\bar{\chi} (\mathcal{D}^+ - g_E \mathcal{K}^+) \chi + \bar{\phi} (\mathcal{D}^- - g_E \mathcal{K}^-) \phi] , \quad (3.8)$$

where the differential operators \mathcal{D}^\pm and the interaction vertices \mathcal{K}^\pm are defined in eqs. (A.5) and (A.6) respectively.

3.3 Fermionic equations of motion

Starting from the action in eq. (3.8), under infinitesimal transformations of the quark fields, we see that, for each flavour, the χ and ϕ fields satisfy the equations of motion

$$i \left\langle [\mathcal{D}^+ - g_E \mathcal{K}^+] \chi(y) O(z) \right\rangle = \left\langle \frac{\delta O(z)}{\delta \bar{\chi}(y)} \right\rangle \quad (3.9)$$

$$i \left\langle [\mathcal{D}^- - g_E \mathcal{K}^-] \phi(y) O(z) \right\rangle = \left\langle \frac{\delta O(z)}{\delta \bar{\phi}(y)} \right\rangle , \quad (3.10)$$

for a generic interpolating field $O(z)$, where the differential operators \mathcal{D}^\pm act on the y coordinates. Analogous equations hold for $\bar{\chi}$ and $\bar{\phi}$. We are interested in the field propagators of χ and ϕ defined as

$$\mathcal{S}_+(x) = S_\chi(x, 0) = \langle \chi(x) \bar{\chi}(0) \rangle_f , \quad \mathcal{S}_-(x) = S_\phi(0, x) = \langle \phi(0) \bar{\phi}(x) \rangle_f , \quad (3.11)$$

where $\langle \cdot \rangle_f$ refers to the expectation value performed by integrating over the fermionic variables only. By choosing $O(z) = \bar{\chi}(z)$, $y = x$ and $z = 0$ and $O(z) = \bar{\phi}(z)$, $y = 0$ and $z = y$ in eqs. (3.9) and (3.10) respectively, the propagators satisfy the equations of motion

$$\left\langle [\mathcal{D}^+ - g_E \mathcal{K}^+] \mathcal{S}_+(x) \right\rangle = -i \mathbb{1} \delta^{(3)}(x) , \quad \left\langle [\mathcal{D}^- - g_E \mathcal{K}^-]^T \mathcal{S}_-(x) \right\rangle = -i \mathbb{1} \delta^{(3)}(x) , \quad (3.12)$$

where $\mathbb{1}$ is the identity in spinor and colour indices, and the transpose acts on the same indices. The expectation values in eq. (3.12) are meant to be taken over the gauge field only, however such equations are also valid at fixed gauge field background.

3.3.1 Perturbative expansion

By setting $g_E = 0$ in the equations of motion, it straightforward to derive their solutions for the quark propagators at tree-level given in Appendix B which read

$$\mathcal{S}_\pm^{(0)}(\mathbf{r}, x_3) = -i \theta(x_3) \mathbb{1} \int_{\mathbf{p}} e^{i\mathbf{p}\cdot\mathbf{r}} e^{-x_3 \left(M + \frac{\mathbf{p}^2}{2\pi T} \right)} , \quad (3.13)$$

where we have shown separately the dependence on the transverse and longitudinal coordinates. At the next-to-leading order, by expanding at $O(g_E)$, the quark propagators read

$$\mathcal{S}_\pm(\mathbf{r}, x_3) = \mathcal{S}_\pm^{(0)}(\mathbf{r}, x_3) + g_E \mathcal{S}_\pm^{(1)}(\mathbf{r}, x_3) + \dots , \quad (3.14)$$

where

$$\mathcal{S}_{\pm}^{(1)}(\mathbf{r}, x_3) = \int_0^{x_3} dz_3 \mathcal{K}^{\pm}\left(\frac{z_3}{x_3}\mathbf{r}, z_3\right) \mathcal{S}_{\pm}^{(0)}(\mathbf{r}, x_3), \quad (3.15)$$

and, as in Ref. [11], in eq. (3.15) we have safely taken that, since quark fields are very heavy, they propagate along the classical trajectory between $(\mathbf{0}, 0)$ and (\mathbf{r}, x_3) . Notice that, at variance of the computations performed in Ref. [11], here the quark propagators at the next-to-leading order are no longer diagonal in Dirac space due to the presence of the non-diagonal term in \mathcal{K}^{\pm} .

4 Mesonic correlators

The expression for the mesonic interpolating fields in the dimensionally reduced effective theory can be promptly derived from eq. (2.1) by using the conventions in Appendix A of Ref. [11] for the Clifford algebra and by employing the three-dimensional representation for the quark fields as in eq. (3.5). Coherently with the choice made for the action, we consider the contributions from the $n = 0$ fermionic Matsubara sector only, and we displace the quark fields in the transverse directions as in Refs. [10, 11], so that

$$\int_0^{1/T} dx_0 \mathcal{O}^a(x_0, x) \rightarrow \mathcal{O}^a(\mathbf{r}_1, \mathbf{r}_2; x_3), \quad (4.1)$$

and the point-split fields read³

$$\mathcal{O}^a(\mathbf{r}_1, \mathbf{r}_2; x_3) = \left[\bar{\chi}(\mathbf{r}_1, x_3) \Sigma_{\mathcal{O}} T^a \phi(\mathbf{r}_2, x_3) - \bar{\phi}(\mathbf{r}_1, x_3) \Sigma_{\mathcal{O}} T^a \chi(\mathbf{r}_2, x_3) \right], \quad (4.2)$$

where from passing from QCD to the effective theory $\Gamma_{\mathcal{O}} = \{\gamma_5, \gamma_2\} \rightarrow \Sigma_{\mathcal{O}} = \{\sigma_3, \sigma_1\}$ for pseudoscalar and vector fields respectively. These fields are not gauge invariant for $\mathbf{r}_1 \neq \mathbf{r}_2$. However, as we will see in the following, the results for the screening masses will be gauge independent, as one can easily prove that gauge dependent contributions in their correlation functions vanish in the large x_3 limit. In the effective field theory, the two-point screening correlation functions introduced in eq. (2.2) map to

$$\mathcal{C}_{\mathcal{O}}(x_3) = \int_{\mathbf{R}} \mathcal{C}_{\mathcal{O}}(\mathbf{r}_1, \mathbf{r}_2; x_3) \Big|_{\mathbf{r}_1=\mathbf{r}_2=\mathbf{R}} = T \int_{\mathbf{R}} \langle \mathcal{O}^a(\mathbf{r}_1, \mathbf{r}_2; x_3) \mathcal{O}^a(0) \rangle \Big|_{\mathbf{r}_1=\mathbf{r}_2=\mathbf{R}}. \quad (4.3)$$

When performing the integration over the fermionic variables and taking the Wick contractions, the quark propagators are diagonal in flavour space. As a consequence, by making explicit the flavour indices, the flavour structure simplifies to $\text{Tr}[T^a T^b] = \delta^{ab}/2$. By considering the latter, and the factor 2 which takes into account the contribution from the $n = -1$ Matsubara sector not explicitly indicated in the previous formulas, the general expression for the correlation functions is

$$\mathcal{C}_{\mathcal{O}}(\mathbf{r}_1, \mathbf{r}_2; x_3) = T \left\langle \text{Tr} \left[\Sigma_{\mathcal{O}} \mathcal{S}_+(\mathbf{r}_1, x_3) \Sigma_{\mathcal{O}} \mathcal{S}_-(\mathbf{r}_2, x_3) \right] \right\rangle = T \left\langle W_{\mathcal{O}}(\mathbf{r}_1, \mathbf{r}_2; x_3) \right\rangle \quad (4.4)$$

where the trace is over colour and spinor indices.

³We use the same symbol for the fields and correlation functions in QCD and in the effective theory since the ambiguity is easily resolved from the context.

4.1 Free-theory limit

The expression of the Wick contraction in the free theory is derived by inserting the propagators in eq. (3.13) into eq. (4.4). By contracting colour and spinor indices, the Wick contraction, independently of the matrix $\Sigma_{\mathcal{O}}$, can be written as

$$\begin{aligned} W_{\mathcal{O}}^{(0)}(\mathbf{r}_1, \mathbf{r}_2; x_3) &= \text{Tr} \left[\mathcal{S}_+^{(0)}(\mathbf{r}_1, x_3) \mathcal{S}_-^{(0)}(\mathbf{r}_2, x_3) \right] \\ &= -2N_c \theta(x_3) \int_{\mathbf{p}_1, \mathbf{p}_2} e^{i(\mathbf{p}_1 \cdot \mathbf{r}_1 + \mathbf{p}_2 \cdot \mathbf{r}_2)} e^{-x_3 \left(2M + \frac{\mathbf{p}_1^2}{2\pi T} + \frac{\mathbf{p}_2^2}{2\pi T} \right)}, \end{aligned} \quad (4.5)$$

and it satisfies the (2+1)-dimensional Schrödinger equation

$$\left[2M + \partial_3 - \sum_{i=1,2} \frac{\nabla_{\mathbf{r}_i}^2}{2\pi T} \right] W_{\mathcal{O}}^{(0)}(\mathbf{r}_1, \mathbf{r}_2; x_3) \stackrel{x_3 \geq 0}{=} 0. \quad (4.6)$$

It follows that, by assuming heavy quarks with small transverse momentum, i.e. longitudinal propagation, the exponential fall-off of $W_{\mathcal{O}}^{(0)}(\mathbf{r}_1, \mathbf{r}_2; x_3)$ is dominated by $2M = 2\pi T + O(g^2)$ which is therefore the leading contribution to both the pseudoscalar and the vector screening masses.

4.2 Next-to-leading order

The next-to-leading order spin-independent correction to the flavour non-singlet mesonic screening masses has been computed, in the framework of the dimensionally-reduced effective theory, in Ref. [10], see eq. (2.4). Here such calculation is extended in order to obtain the leading spin-dependent correction to the screening masses. Starting from the equations of motion for the quark propagators in eq. (3.12), the equation of motion for $\langle W_{\mathcal{O}} \rangle$ in the interacting case reads

$$\begin{aligned} &\left[2M + \partial_3 - \sum_{i=1,2} \frac{\nabla_{\mathbf{r}_i}^2}{2\pi T} \right] \langle W_{\mathcal{O}}(\mathbf{r}_1, \mathbf{r}_2; x_3) \rangle \stackrel{x_3 \geq 0}{=} \\ &\stackrel{x_3 \geq 0}{=} g_E \left\langle \text{Tr} \left\{ \left[\mathcal{A}^+(\mathbf{r}_1, x_3) + \mathcal{A}^-(\mathbf{r}_2, x_3) \right] \Sigma_{\mathcal{O}} \mathcal{S}_+(\mathbf{r}_1, x_3) \Sigma_{\mathcal{O}} \mathcal{S}_-(\mathbf{r}_2, x_3) \right\} \right. \\ &\quad \left. - \frac{1}{2\pi T} \text{Tr} \left\{ \left[s_{\mathcal{O}} B_3(\mathbf{r}_1, x_3) + B_3(\mathbf{r}_2, x_3) \right] \sigma_3 \Sigma_{\mathcal{O}} \mathcal{S}_+(\mathbf{r}_1, x_3) \Sigma_{\mathcal{O}} \mathcal{S}_-(\mathbf{r}_2, x_3) \right\} \right\rangle. \end{aligned} \quad (4.7)$$

where \mathcal{A}^{\pm} is defined in eq. (A.2), and we have introduced the notation $s_{\mathcal{O}} = (+1, -1)$ for pseudoscalar and vector respectively, see Appendix C. By using the quark propagators at $O(g_E)$ in eq. (3.14), and by performing the gluon contractions (see Appendix C for further details) we obtain

$$\left[2M + \partial_3 - \sum_{i=1,2} \frac{\nabla_{\mathbf{r}_i}^2}{2\pi T} \right] \langle W_{\mathcal{O}}(\mathbf{r}_1, \mathbf{r}_2; x_3) \rangle \stackrel{x_3 \geq 0}{=} -\mathcal{U}(\mathbf{r}_1, \mathbf{r}_2; x_3) W_{\mathcal{O}}^{(0)}(\mathbf{r}_1, \mathbf{r}_2; x_3) + O(g_E^3), \quad (4.8)$$

where the potential is

$$\mathcal{U}(\mathbf{r}_1, \mathbf{r}_2; x_3) = \mathcal{U}_{\text{SI}_1}(\mathbf{r}_1, \mathbf{r}_2; x_3) + \mathcal{U}_{\text{SI}_2}(\mathbf{r}_1, \mathbf{r}_2; x_3) + \mathcal{U}_{\mathcal{O}}(\mathbf{r}_1, \mathbf{r}_2; x_3), \quad (4.9)$$

with

$$\mathcal{U}_{\text{SI}_1}(\mathbf{r}_1, \mathbf{r}_2; x_3) = -\frac{g_E^2}{N_c} \left\langle \text{Tr} \left\{ \left[\mathcal{A}^+(\mathbf{r}_1, x_3) + \mathcal{A}^-(\mathbf{r}_2, x_3) \right] \times \int_0^{x_3} dz_3 \left[\mathcal{A}^+\left(\frac{z_3}{x_3} \mathbf{r}_1, z_3\right) + \mathcal{A}^-\left(\frac{z_3}{x_3} \mathbf{r}_2, z_3\right) \right] \right\} \right\rangle, \quad (4.10)$$

$$\mathcal{U}_{\text{SI}_2}(\mathbf{r}_1, \mathbf{r}_2; x_3) = -\frac{g_E^2}{(2\pi T)^2 N_c} \times \int_0^{x_3} dz_3 \left\langle \text{Tr} \left\{ B_3(\mathbf{r}_1, x_3) B_3\left(\frac{z_3}{x_3} \mathbf{r}_1, z_3\right) + B_3(\mathbf{r}_2, x_3) B_3\left(\frac{z_3}{x_3} \mathbf{r}_2, z_3\right) \right\} \right\rangle, \quad (4.11)$$

and the chromo-magnetic field B_3 is defined at leading order in eq. (A.4). The $\mathcal{U}_{\text{SI}_1}$ potential is the one that was obtained in Ref. [10]. The second spin-independent contribution $\mathcal{U}_{\text{SI}_2}$ is temperature suppressed. It derives from the exchange of longitudinal ultrasoft gluons along the same quark line. The leading contribution to the spin-dependent potential reads

$$\mathcal{U}_{\mathcal{O}}(\mathbf{r}_1, \mathbf{r}_2; x_3) = -\frac{g_E^2 s_{\mathcal{O}}}{(2\pi T)^2 N_c} \times \int_0^{x_3} dz_3 \left\langle \text{Tr} \left\{ B_3(\mathbf{r}_1, x_3) B_3\left(\frac{z_3}{x_3} \mathbf{r}_2, z_3\right) + B_3(\mathbf{r}_2, x_3) B_3\left(\frac{z_3}{x_3} \mathbf{r}_1, z_3\right) \right\} \right\rangle. \quad (4.12)$$

It is temperature suppressed, and it is due to the exchange of ultrasoft gluons between two quark lines. Since to extract the screening masses we are interested in the large x_3 behaviour of the Wick contractions in eq. (4.4), we take the limit $x_3 \rightarrow \infty$ in eq. (4.8) which reads

$$\left[2M + \partial_3 - \sum_{i=1,2} \frac{\nabla_{\mathbf{r}_i}^2}{2\pi T} + U(\mathbf{r}_1 - \mathbf{r}_2) \right] \langle W_{\mathcal{O}}(\mathbf{r}_1, \mathbf{r}_2; x_3) \rangle = 0 + O(g_E^3), \quad (4.13)$$

where

$$U(\mathbf{r}_1 - \mathbf{r}_2) = \lim_{x_3 \rightarrow \infty} \left[\mathcal{U}_{\text{SI}_1}(\mathbf{r}_1, \mathbf{r}_2; x_3) + \mathcal{U}_{\text{SI}_2}(\mathbf{r}_1, \mathbf{r}_2; x_3) + \mathcal{U}_{\mathcal{O}}(\mathbf{r}_1, \mathbf{r}_2; x_3) \right], \quad (4.14)$$

and, at the order we work, we could replace $W_{\mathcal{O}}^{(0)} \rightarrow \langle W_{\mathcal{O}} \rangle$.

4.2.1 Spin-independent contribution

The spin-independent contribution $\mathcal{U}_{\text{SI}_2}$ in eq. (4.11) is temperature-suppressed with respect to the one in eq. (4.10), and it can be neglected when keeping terms up to $O(g_E^2/T)$ only. By taking into account the discussion in Section 5, this potential would produce subleading contributions in the wave-functions of the screening mass states, and therefore in the hyperfine splitting. Similarly, since we are interested in the leading contribution to eq. (2.5) only, we can safely take the expression of the low energy constant M in eq. (3.6). By taking the large separation limit of the potential in eq. (4.10), see Appendix D for the intermediate steps, we obtain for the next-to-leading spin-independent contribution

$$U_{\text{SI}_1}(\mathbf{r}) = \lim_{x_3 \rightarrow \infty} \mathcal{U}_{\text{SI}_1}(\mathbf{r}_1, \mathbf{r}_2; x_3) = \frac{g_E^2 C_F}{2\pi} \left[\ln\left(\frac{m_E r}{2}\right) + \gamma_E - K_0(m_E r) \right] \quad (4.15)$$

where $\mathbf{r} = \mathbf{r}_1 - \mathbf{r}_2$ and $r = |\mathbf{r}|$, γ_E is the Euler-Mascheroni constant and K_0 is a modified Bessel function. Note that the leading logarithmic behaviour on the r.h.s. of eq. (4.15) is a confining Coulomb interaction in $2 + 1$ dimensions. By combining the power counting reported in Ref. [11] and standard dimensional analysis arguments, it is possible to see that a string term, i.e. a non-perturbative confining term, arises in the potential at $O(g^3)$. This limits, de facto, the applicability of the perturbative approach for computing the spin-independent potential to the $O(g^2)$.

4.2.2 Spin-dependent contribution

The explicit expression for the spin-dependent static potential $U_{\mathcal{O}}$ in eq. (4.12) is carried out analogously, see Appendix D for the intermediate steps and the detailed calculations. By taking the large separation limit in the longitudinal direction, it yields to

$$U_{\mathcal{O}}(\mathbf{r}) = \lim_{x_3 \rightarrow \infty} \mathcal{U}_{\mathcal{O}}(\mathbf{r}_1, \mathbf{r}_2; x_3) = -g_E^2 \frac{s_{\mathcal{O}} C_F}{(2\pi T)^2} \delta^{(2)}(\mathbf{r}). \quad (4.16)$$

Notice that, while it provides an interaction which is of the same order in the effective coupling constant g_E with respect to the spin-independent potential in eq. (4.15), it is however temperature-suppressed.

5 Hyperfine splitting

As we have seen in the previous section, the equation of motion for the two-point mesonic screening correlator in the three-dimensional effective theory implies the Schrödinger equation in eq. (4.13), and the screening mass corresponds to its ground-state energy. Since the spin-dependent potential in eq. (4.16) provides a temperature-suppressed contribution with respect to the leading spin-independent potential in eq. (4.15), $U_{\mathcal{O}}(\mathbf{r})$ can be treated as a perturbative correction. We then start by solving the unperturbed Schrödinger equation, which, in the large x_3 limit, reads

$$\left[-\frac{\nabla_{\mathbf{r}_1}^2 + \nabla_{\mathbf{r}_2}^2}{2\pi T} + 2M + U_{\text{SI}_1}(\mathbf{r}_1 - \mathbf{r}_2) \right] \Psi_0(\mathbf{r}_1, \mathbf{r}_2) = E_0 \Psi_0(\mathbf{r}_1, \mathbf{r}_2), \quad (5.1)$$

where, with Ψ_0 and E_0 , we refer to the ground-state energy and wave-function at leading order in perturbation theory⁴. By going to the center-of-mass frame, we define

$$\mathbf{R} = \frac{\mathbf{r}_1 + \mathbf{r}_2}{2}, \quad \mathbf{r} = \mathbf{r}_1 - \mathbf{r}_2, \quad (5.2)$$

and the Laplace operator can accordingly be written as

$$\nabla_{\mathbf{r}_1}^2 + \nabla_{\mathbf{r}_2}^2 = \frac{1}{2} \nabla_{\mathbf{R}}^2 + 2 \nabla_{\mathbf{r}}^2, \quad (5.3)$$

where the first term on the r.h.s. describes the motion of the center-of-mass, while the second one is the kinetic term related to the relative motion. By restricting to the relative

⁴In this section we omit any label referring to the eigenstates of the Hamiltonian since we are only interested in the ground state of the system.

motion only, and by making explicit the functional form of the potential, see eq. (4.15), the spin-independent Schrödinger equation reads

$$\left\{ -\frac{\nabla_{\mathbf{r}}^2}{\pi T} + 2M + g_{\mathbb{E}}^2 \frac{C_F}{2\pi} \left[\ln\left(\frac{m_{\mathbb{E}} r}{2}\right) + \gamma_{\mathbb{E}} - K_0(m_{\mathbb{E}} r) \right] - E_0 \right\} \psi_0(\mathbf{r}) = 0, \quad (5.4)$$

This is exactly the Schrödinger equation obtained in Ref. [10] which leads the next-to-leading order value of the mesonic screening mass in eq. (2.4). Once E_0 and the normalized ψ_0 have been determined for the unperturbed Schrödinger equation, the mesonic screening masses at the first order in the spin-dependent perturbative expansion reads

$$E_{\mathcal{O}} = E_0 + \int_{\mathbf{r}} U_{\mathcal{O}}(\mathbf{r}) |\psi_0(\mathbf{r})|^2 = E_0 - g_{\mathbb{E}}^2 \frac{s_{\mathcal{O}} C_F}{(2\pi T)^2} |\psi_0(\mathbf{0})|^2. \quad (5.5)$$

It is important to notice that, even though the spin-dependent potential is localized in $\mathbf{r} = 0$, the hyperfine correction to the screening masses receives contributions from large distances through the normalization of the wave-function, see discussion below.

5.1 Leading contribution

The solution of the spin-independent eigenvalue problem for the ground state is found by going to polar coordinates, and by considering the case of vanishing angular momentum. By defining $\hat{\psi}_0(\hat{r}) = \psi_0(\mathbf{r}) \sqrt{2\pi}/m_{\mathbb{E}}$, where we introduced the dimensionless variable $\hat{r} = m_{\mathbb{E}} r$, Eq. (5.1) can then be rewritten as

$$\left\{ -\left(\frac{d^2}{d\hat{r}^2} + \frac{1}{\hat{r}} \frac{d}{d\hat{r}} \right) + \rho \left[\ln\left(\frac{\hat{r}}{2}\right) + \gamma_{\mathbb{E}} - K_0(\hat{r}) - \hat{E}_0 \right] \right\} \hat{\psi}_0(\hat{r}) = 0. \quad (5.6)$$

Accordingly to Ref. [10], we introduced the parameterization of the effective coupling

$$\rho = \frac{g_{\mathbb{E}}^2 C_F T}{2m_{\mathbb{E}}^2} = \frac{4}{9}, \quad (5.7)$$

where in the last step we used $N_f = 3$, $N_c = 3$ and the expressions at leading order for $m_{\mathbb{E}}$ and $g_{\mathbb{E}}^2$ reported in eq. (3.2). Furthermore we introduced the dimensionless energy eigenvalue [10]

$$\hat{E}_0 = \frac{2\pi}{g_{\mathbb{E}}^2 C_F} (E_0 - 2M). \quad (5.8)$$

By doing the same change of variable in the matrix element of the spin-dependent potential and in the normalization of the wave-function, the spin-dependent eigenvalue in eq. (5.5) can be written as

$$E_{\mathcal{O}} = E_0 - \frac{g_{\mathbb{E}}^2 m_{\mathbb{E}}^2}{2\pi} \frac{s_{\mathcal{O}} C_F}{(2\pi T)^2} |\hat{\psi}_0(0)|^2, \quad (5.9)$$

where

$$\int_0^\infty d\hat{r} \hat{r} |\hat{\psi}_0(\hat{r})|^2 = 1. \quad (5.10)$$

By recalling that $s_{\mathcal{O}} = (+1, -1)$ for the pseudoscalar and the vector correlators respectively, and by inserting the expression at leading order for $m_{\mathbb{E}}^2$ and $g_{\mathbb{E}}^2$, see eq. (3.2), it follows that the hyperfine-splitting in the pseudoscalar and vector energy levels due to spin-dependent interactions at leading order in perturbation theory, cf. eq. (2.5), is

$$\frac{\Delta m_{\text{VP}}^{\text{lo}}}{2\pi T} = g^4 \left(\frac{N_c}{3} + \frac{N_f}{6} \right) \frac{C_F}{8\pi^4} |\hat{\psi}_0(0)|^2, \quad (5.11)$$

where we substituted $E_{\text{P}} = m_{\text{P}}$ and $E_{\text{V}} = m_{\text{V}}$ in eq. (5.9). The numerical solution for $\hat{\psi}_0$ of the unperturbed Schrödinger equation (5.6) gives

$$\frac{\Delta m_{\text{VP}}^{\text{lo}}}{2\pi T} = 0.002376 \cdot g^4. \quad (5.12)$$

This result justifies a posteriori the choice of neglecting $O(g_{\mathbb{E}}^2/T^2)$ terms in the spin-independent potential in Section 4.2.1, since it is clear that the inclusion of the potential obtained from eq. (4.11) into eq. (5.1) would have produced higher order effects in the spin-splitting between the pseudoscalar and the vector screening masses. A similar discussion holds for the higher order contributions deriving from the perturbative matching between the three-dimensional non-relativistic theory in eq. (3.5) and QCD. From the discussion in Section 4.2.1, a string term of non-perturbative origin starts at $O(g^3)$ in the static potential, and, as a consequence, non-perturbative effects are expected to start contributing to the hyperfine splitting at $O(g^5)$. Therefore, to go beyond the result in eq. (5.11), a non-perturbative approach is required.

5.2 Analysis of the wave-function

The perturbative result for the hyperfine-splitting in eq. (5.11) probes the normalized wave function of the quark-antiquark bound system at the origin. In particular its normalization takes contributions from all distances, and therefore from both the scales present in EQCD, i.e. $r \sim m_{\mathbb{E}}^{-1}$ and $(g^2 T)^{-1}$. To scrutinize this issue, it is interesting to define the probability

$$P(\hat{r}_{\text{np}}) = \int_0^{\hat{r}_{\text{np}}} d\hat{r} \hat{r} |\hat{\psi}_0(\hat{r})|^2, \quad (5.13)$$

for the quark-antiquark pair to be at a distance $\hat{r} \leq \hat{r}_{\text{np}}$, where

$$\hat{r}_{\text{np}} = m_{\mathbb{E}} r_{\text{np}} = \frac{m_{\mathbb{E}}}{g_{\mathbb{E}}^2} = \left(\frac{N_c}{3} + \frac{N_f}{6} \right)^{1/2} \frac{1}{g} = \sqrt{\frac{3}{2}} \frac{1}{g}, \quad (5.14)$$

and on the r.h.s. we substituted $N_f = 3$ and $N_c = 3$ which is the relevant case to this study. In Figure 1 we show the probability density as a function of \hat{r} together with the ratio \hat{r}_{np} of the two relevant scales (dashed line). As expected, at asymptotically high temperatures (left panel) the probability for the quark and the antiquark to be at distances $\hat{r} \leq \hat{r}_{\text{np}}$ is close to 1 (blue band), and the perturbative determination in eq. (5.11) becomes more and more reliable as the temperature increases. In the central and right panels of Figure 1 the cases for $T \sim 4 \times 10^8$ GeV ($P(\hat{r}_{\text{np}}) \sim 70\%$) and for $T \sim \times 10^2$ GeV ($P(\hat{r}_{\text{np}}) \sim 40\%$) are

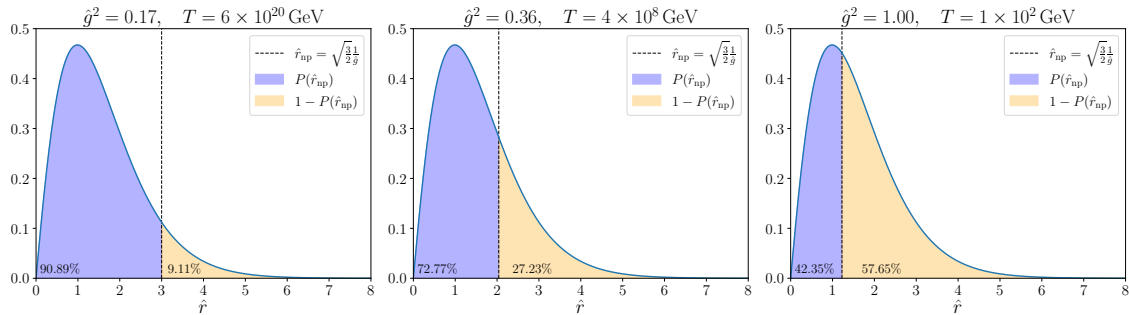


Figure 1. Probability density for the quark-antiquark pair as a function of the distance \hat{r} . The probability for the quark and the antiquark to be at distances $\hat{r} \leq \hat{r}_{\text{np}}$, see eq. (5.13), is indicated by the blue area for different values of the coupling constant (temperature), with the latter increasing from left to right. As the temperature decreases, the blue area becomes larger and larger.

shown, respectively. It is rather clear that, at temperatures of the order of the electro-weak scale, the probability for the quark and the antiquark to be at distances larger than \hat{r}_{np} approaches 50%. As a consequence, long-distance (ultra-soft) contributions are relevant, and non-perturbative effects must be taken into account. As discussed previously, they start contributing already at $O(g^5)$ for the hyperfine splitting.

This analysis, albeit rather crude, is consistent with the fact that the hierarchy of scales in eq. (3.4) sets in only at much higher temperatures with respect to the electro-weak scale, where $g \sim 1$. The result in eq. (5.11), however, remains extremely useful to discriminate, among the possible interpolating fit functions of the non-perturbative data, those which have the correct asymptotic behaviour at asymptotically large temperatures.

6 Comparison with non-perturbative results

The flavour non-singlet pseudoscalar and vector screening masses have been computed recently in thermal QCD with $N_f = 3$ massless quarks in the range of temperatures from $T \sim 1$ GeV up to ~ 160 GeV with high precision [7]. By remembering that $m_P = E_P$ and $m_V = E_V$, where the expressions for E_P and E_V are given in eq. (5.9), it follows that the magnitude of the leading spin-dependent correction is the same for both masses, but with opposite sign. Therefore, up to $O(g^4)$, the sum of the pseudoscalar and the vector screening masses probes the spin-independent potential only. In the two panels of Figure 2 we report the non-perturbative data for $(m_V + m_P)/4\pi T$ from Ref. [7] as a function of \hat{g} , the renormalized coupling in the $\overline{\text{MS}}$ scheme at two-loop order evaluated at the renormalization scale $\mu = 2\pi T$, see eq. (7.1) of Ref. [7] for its precise definition. We stress once again that, for our purposes, \hat{g} is just a function of the temperature T , suggested by the effective theory analysis, that we use to analyze the non-perturbative data. The crucial point is its leading logarithmic dependence on T . In the left panel of Figure 2 the bending down of the normalized sum of the the two masses as the temperature decreases signals the presence of higher order contributions with respect to the leading interacting term in eq. (2.4). Data exhibit a very mild temperature dependence which is originated by the competition

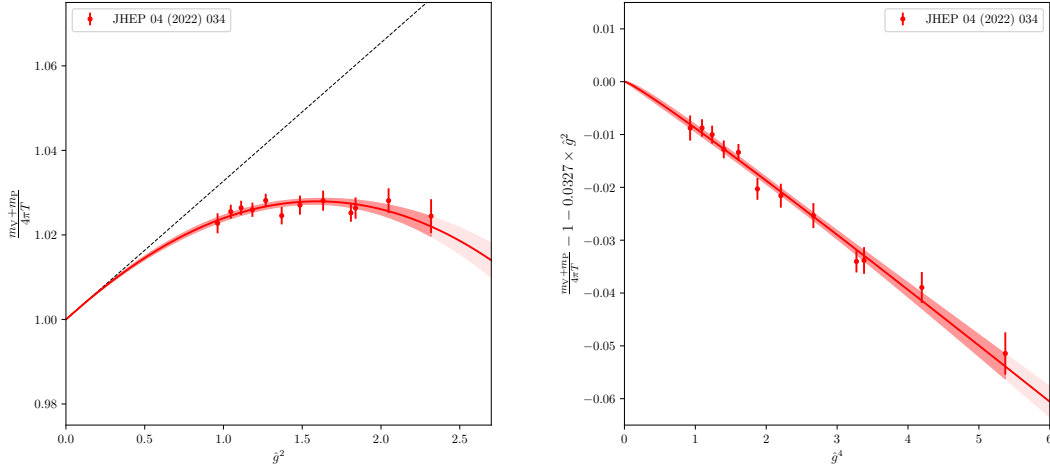


Figure 2. Left: sum of the pseudoscalar and the vector screening masses, normalized to $4\pi T$, as a function of \hat{g}^2 . Lattice data are obtained from Ref. [7], the red band represents the best parameterization in eq. (6.1) with its error, while the black dashed line is the analytically known spin-independent contribution in eq. (2.4). Right: same as in the left panel but with the lattice data, subtracted by the analytically known contribution, plotted versus \hat{g}^4 .

between the leading contribution in eq. (2.4) and higher order corrections. This results in a positive correction of about 2% with respect to the free field theory result in the entire range of temperature explored. In the right panel of Figure 2 we show the normalized sum of the two masses after subtracting the known leading contribution in eq. (2.4), plotted as a function of \hat{g}^4 . At the highest temperature, i.e. $\hat{g}^4 \sim 1$, higher order terms provide a contribution which is still about 30% of the leading interacting term, while at $T \sim 1$ GeV, i.e. $\hat{g}^4 \sim 5$, this contribution increases up to $\sim 70\%$. Given these considerations, we parameterize the non-perturbative data with the polynomial

$$\frac{m_V + m_P}{4\pi T} = p_0 + p_2 \hat{g}^2 + p_3 \hat{g}^3 + p_4 \hat{g}^4. \quad (6.1)$$

A fit of the data reveals that the leading and the quadratic coefficients p_0 and p_2 turns out to be compatible with the free field theory and the leading perturbative interacting contributions respectively, see eq. (2.4). We thus enforce $p_0 = 1$ and $p_2 = 0.032740$, and fit the data again. As a result, we obtain, for the remaining fit parameters, $p_3 = 0.0036(29)$ and $p_4 = -0.0124(23)$, with $\text{cov}(p_3, p_4) / [\sigma(p_3)\sigma(p_4)] = -0.99$ and $\chi^2/\text{d.o.f.} = 0.60$. Given the high quality of this fit, we take this as final parameterization of the lattice data, and we display it as a red band in both panels of Figure 2. For completeness, let us notice that, by enforcing $p_3 = 0$, we obtain $p_4 = -0.00959(27)$ and, again, an excellent $\chi^2/\text{d.o.f.} = 0.69$. These findings show that the data in Ref. [7] are compatible with the expected behaviour at asymptotically large temperatures, but higher order terms in \hat{g} are required to explain their temperature dependence. Since non-perturbative contributions are expected already at $O(g^3)$, they have to be taken into account for explaining the results in Figure 2 up to

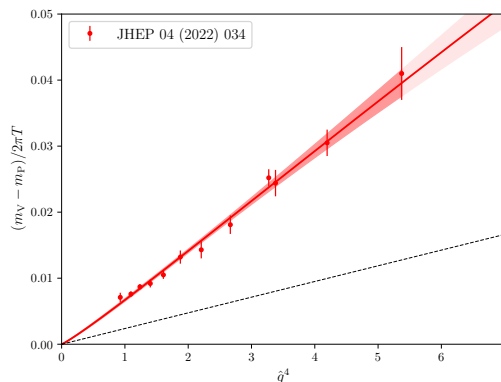


Figure 3. Difference of the vector and pseudoscalar screening masses normalized to $2\pi T$ versus \hat{g}^4 . The perturbative result in eq. (5.12) is the dashed black line, while the red curve represents the fit in eq. (6.2).

temperatures of the order of the electro-weak scale.

The spin-dependent contribution to the mesonic screening masses has been determined in Ref. [7] from the mass difference of m_V and m_P . The results are reported in Figure 3 as a function of \hat{g}^4 . Within statistical errors, data show an effective quartic dependence on \hat{g} in the entire range of temperature explored. However, the effective slope, 0.00704(14), turns out to be approximately 3 times the coefficient on the r.h.s. of eq. (5.12). Thanks to the perturbative result in eq. (5.12), however, we can constrain the asymptotic behaviour of the mass difference between the vector and the pseudoscalar screening masses at asymptotically large temperatures. We then parameterize the non-perturbative data in Ref. [7] as

$$\frac{m_V - m_P}{2\pi T} = 0.002376 \hat{g}^4 + s_5 \hat{g}^5 + s_6 \hat{g}^6, \quad (6.2)$$

where a fit to the data gives $s_5 = 0.0063(9)$, $s_6 = -0.0020(7)$, $\text{cov}(s_5, s_6) / [\sigma(s_5)\sigma(s_6)] = -0.99$, and an excellent $\chi^2/\text{d.o.f.} = 0.75$. The eq. (6.2) represents our best parameterization of the non-perturbative data. Being s_5 about 3 times in magnitude with respect to s_4 , it follows that the leading $O(\hat{g}^4)$ term accounts only for a small fraction of the total contribution in the entire range of temperatures studied in Ref. [7]. The bulk of the hyperfine splitting originates from higher order terms which can be present both in the spin-dependent potential and in the unperturbed, spin-independent wave-function. As a result contributions of non-perturbative origin has to be taken into account to explain the observed magnitude of the hyperfine splitting up to the electro-weak scale. This does not come as a surprise given the analysis in section 5.2.

7 Conclusions

Recent progress in lattice QCD has made it possible to study the strongly interacting quark gluon plasma non-perturbatively up to temperatures of the order of the electro-weak scale. First results indicate that non-perturbative contributions needs to be considered up

to temperatures orders of magnitude larger than the GeV scale to explain the dynamics of the theory. Of particular interest is the hyperfine splitting in the QCD flavour non-singlet mesonic screening masses because it can be computed very precisely on the lattice and it is expected to be particularly sensitive to non-perturbative dynamics.

Motivated by the results in Ref. [7], here we have computed analytically the leading contribution of $O(g^4)$ to the hyperfine splitting at asymptotically large temperatures. Non-perturbative data indeed show an effective $O(g^4)$ behaviour [7], within statistical errors, in the temperature range from $T \sim 1$ GeV up to 160 GeV. The effective prefactor, however, is approximately 3 times larger than the one of the leading $O(g^4)$ contribution at asymptotically high temperatures. By enforcing the $O(g^4)$ term to its analytic value in eq. (5.12), non-perturbative data for the hyperfine splitting are compatible with the presence of large contributions from higher orders up to the highest temperature considered.

In the temperature range explored, the origin of these terms can be traced back to higher order effects either in the spin-dependent potential or in the spin-independent wavefunction. In the latter case the true wave function of the screening state would be more peaked at the origin, which in turn implies a stronger binding potential with respect to the leading one of $O(g^2)$ in eq. (5.4). Since the $O(g^3)$ term in the potential takes contribution of non-perturbative origin [1], a higher order calculation of both the spin-independent screening masses and the hyperfine splitting has to take into account non-perturbative contributions.

From a more theoretical point of view, these results call for non-perturbative computations in the three-dimensional theory in order to match the effective theory with QCD non-perturbatively. This will allow to shed light on the origin of the various contributions, and to verify non-perturbatively the effective theory paradigm. At the same time, the possibility of studying QCD at high temperatures by Monte Carlo simulations, makes the effective theory analysis less compelling especially if higher and higher orders must be taken into account.

Shortly before we completed the writing of this paper, a study has been published on arXiv [25] which addresses the same topic studied here. In particular the authors explore the effects of including non-perturbative contributions in the spin-independent potential to explain the hyperfine splitting observed in Ref. [7].

Acknowledgements

We wish to thank Mikko Laine for several discussions on the topics of this paper. This work is partially supported by ICSC – Centro Nazionale di Ricerca in High Performance Computing, Big Data and Quantum Computing, funded by European Union – NextGenerationEU. The research of M.C. is funded through the MUR program for young researchers “Rita Levi Montalcini”. D.L. is supported by ERC grant StrangeScatt-101088506.

A Simplification of the fermionic action

For the computation of the leading contribution to the hyperfine splitting in the mesonic screening masses, the action in eq. (3.5) can be further simplified and written in a more compact way. In particular, we can safely neglect the interacting terms appearing in the transverse covariant derivative D_\perp because they would produce either spin-independent or sub-leading spin-dependent contributions. For each flavour, the action in eq. (3.5) can then be written as

$$S_{\text{NRQCD}} = i \int d^3x \left\{ \bar{\chi} \left[M + \partial_3 - g_E \mathcal{A}^+ - \frac{1}{2\pi T} \left(\nabla_\perp^2 + \frac{g_E}{4i} [\sigma_j, \sigma_k] F_{jk} \right) \right] \chi \right. \\ \left. + \bar{\phi} \left[M - \partial_3 - g_E \mathcal{A}^- - \frac{1}{2\pi T} \left(\nabla_\perp^2 + \frac{g_E}{4i} [\sigma_j, \sigma_k] F_{jk} \right) \right] \phi \right\} + \dots, \quad (\text{A.1})$$

where we introduced the spin-independent vertex operator \mathcal{A}^\pm defined as

$$\mathcal{A}^\pm = \mathcal{A}^{\pm, \lambda} T^\lambda = \left(A_0^\lambda \pm i A_3^\lambda \right) T^\lambda, \quad \lambda = 1, \dots, N_c^2 - 1. \quad (\text{A.2})$$

Furthermore, by recalling that $[\sigma_j, \sigma_k] = 2i\epsilon_{jkl}\sigma_l$ and since we are only interested in $j, k = 1, 2$ and therefore $l = 3$, the spin-dependent term in the action can be readily written as

$$[\sigma_j, \sigma_k] F_{jk} = -4i\sigma_3 B_3, \quad (\text{A.3})$$

where the chromo-magnetic field is defined as

$$B_3 = - \left[\partial_1 A_2 - \partial_2 A_1 \right] + O(g_E), \quad (\text{A.4})$$

and we can safely neglect $O(g_E)$ terms since we are only interested in the leading spin-dependent corrections. By introducing the differential operators

$$\mathcal{D}^\pm = M \pm \partial_3 - \frac{\nabla_\perp^2}{2\pi T}, \quad (\text{A.5})$$

and the interaction vertices

$$\mathcal{K}^\pm(x) = \mathcal{K}^{\pm, \lambda}(x) T^\lambda = \left(\mathcal{A}^{\pm, \lambda}(x) \mathbb{1} - \frac{1}{2\pi T} \sigma_3 B_3^\lambda(x) \right) T^\lambda, \quad (\text{A.6})$$

with $\mathbb{1}$ being the identity matrix in the spin indices, the NRQCD action can be written in the compact way given in eq. (3.8).

B Propagators in the free theory

In this appendix we define the free propagators for the fields entering the actions S_{EQCD} and S_{NRQCD} in eqs. (3.1) and (3.5), respectively. By setting $g_E = 0$ in these actions, the free-theory gauge field propagators read

$$\left\langle A_\mu^\lambda(x) A_\nu^\rho(0) \right\rangle_0 = \delta^{\lambda\rho} \Delta_{\mu\nu}(x), \quad (\text{B.1})$$

where $\mu, \nu = 0, \dots, 3$, $\lambda, \rho = 1, \dots, N_c^2 - 1$ and in the Feynman gauge it holds

$$\Delta_{\mu\nu}(x) = \delta_{\mu\nu} \int \frac{d^3p}{(2\pi)^3} e^{ip \cdot x} \left[\frac{\delta_{\mu 0}}{p^2 + m_E^2} + \frac{\delta_{\mu i}}{p^2} \right], \quad (\text{B.2})$$

with m_E being defined in eq. (3.2), and $i = 1, 2, 3$. The quark propagators at tree-level are defined as

$$\langle \chi(x) \bar{\chi}(0) \rangle_0 = S_\chi^{(0)}(x, 0), \quad \langle \phi(x) \bar{\phi}(0) \rangle_0 = S_\phi^{(0)}(x, 0), \quad (\text{B.3})$$

where

$$S_\chi^{(0)}(x, 0) = S_\phi^{(0)}(0, x) = -i\theta(x_3) \mathbb{1} \int_{\mathbf{p}} e^{i\mathbf{p} \cdot \mathbf{r}} e^{-x_3 \left(M + \frac{\mathbf{p}^2}{2\pi T} \right)}, \quad x = (\mathbf{r}, x_3), \quad (\text{B.4})$$

and $\mathbb{1}$ is the identity in spinor and colour indices. The integration over the transverse momenta is defined as $\int_{\mathbf{p}} = \int d^2\mathbf{p}/(2\pi)^2$.

C Equations of motion at next-to-leading order

In this appendix we report the intermediate steps to obtain eq. (4.8) from eq. (4.7). By inserting eq. (3.14) into the r.h.s. of eq. (4.7), we obtain

$$\begin{aligned} \left[2M + \partial_3 - \sum_{i=1,2} \frac{\nabla_{\mathbf{r}_i}^2}{2\pi T} \right] \langle W_{\mathcal{O}}(\mathbf{r}_1, \mathbf{r}_2; x_3) \rangle &= g_E^2 \left\langle \text{Tr} \left\{ \left[\mathcal{A}^+(\mathbf{r}_1, x_3) + \mathcal{A}^-(\mathbf{r}_2, x_3) \right] \right. \right. \\ &\left. \left[\Sigma_{\mathcal{O}} \mathcal{S}_+^{(0)}(\mathbf{r}_1, x_3) \Sigma_{\mathcal{O}} \mathcal{S}_-^{(1)}(\mathbf{r}_2, x_3) + \Sigma_{\mathcal{O}} \mathcal{S}_+^{(1)}(\mathbf{r}_1, x_3) \Sigma_{\mathcal{O}} \mathcal{S}_-^{(0)}(\mathbf{r}_2, x_3) \right] \right\} - \frac{1}{2\pi T} \text{Tr} \left\{ \left[s_{\mathcal{O}} B_3(\mathbf{r}_1, x_3) \right. \right. \\ &\left. \left. + B_3(\mathbf{r}_2, x_3) \right] \sigma_3 \left[\Sigma_{\mathcal{O}} \mathcal{S}_+^{(0)}(\mathbf{r}_1, x_3) \Sigma_{\mathcal{O}} \mathcal{S}_-^{(1)}(\mathbf{r}_2, x_3) + \Sigma_{\mathcal{O}} \mathcal{S}_+^{(1)}(\mathbf{r}_1, x_3) \Sigma_{\mathcal{O}} \mathcal{S}_-^{(0)}(\mathbf{r}_2, x_3) \right] \right\} \Bigg\rangle + O(g_E^3). \end{aligned} \quad (\text{C.1})$$

By inserting the expression for the quark propagators at next-to-leading order in eq. (3.15) and by recalling that, given the expression for \mathcal{K}^\pm in eq. (A.6), \mathcal{A}^\pm only contracts with \mathcal{A}^\pm and B_3 only with B_3 , the equation of motion can be written as

$$\begin{aligned} \left[2M + \partial_3 - \sum_{i=1,2} \frac{\nabla_{\mathbf{r}_i}^2}{2\pi T} \right] \langle W_{\mathcal{O}}(\mathbf{r}_1, \mathbf{r}_2; x_3) \rangle &= \frac{g_E^2}{N_c} W_{\mathcal{O}}^{(0)}(\mathbf{r}_1, \mathbf{r}_2; x_3) \times \\ &\left\{ \left\langle \text{Tr} \left\{ \left[\mathcal{A}^+(\mathbf{r}_1, x_3) + \mathcal{A}^-(\mathbf{r}_2, x_3) \right] \int_0^{x_3} dz_3 \left[\mathcal{A}^+\left(\frac{z_3}{x_3} \mathbf{r}_1, z_3\right) + \mathcal{A}^-\left(\frac{z_3}{x_3} \mathbf{r}_2, z_3\right) \right] \right\} \right\} + \right. \\ &\frac{1}{(2\pi T)^2} \int_0^{x_3} dz_3 \left\langle \text{Tr} \left\{ B_3(\mathbf{r}_1, x_3) B_3\left(\frac{z_3}{x_3} \mathbf{r}_1, z_3\right) + B_3(\mathbf{r}_2, x_3) B_3\left(\frac{z_3}{x_3} \mathbf{r}_2, z_3\right) \right\} \right\rangle + \\ &\left. \frac{s_{\mathcal{O}}}{(2\pi T)^2} \int_0^{x_3} dz_3 \left\langle \text{Tr} \left\{ B_3(\mathbf{r}_1, x_3) B_3\left(\frac{z_3}{x_3} \mathbf{r}_2, z_3\right) + B_3(\mathbf{r}_2, x_3) B_3\left(\frac{z_3}{x_3} \mathbf{r}_1, z_3\right) \right\} \right\rangle \right\} + O(g_E^3), \end{aligned} \quad (\text{C.2})$$

where the tree-level value $W_{\mathcal{O}}^{(0)}(\mathbf{r}_1, \mathbf{r}_2; x_3)$ is defined in eq. (4.5), and we have introduced $s_{\mathcal{O}} = (+1, -1)$ for the pseudoscalar and the vector fields respectively. Moreover we have exploited the fact that, when contracting the gauge fields $\langle \mathcal{A}^{\pm, \rho} \mathcal{A}^{\pm, \lambda} \rangle \propto \delta^{\rho\lambda}$ and $\langle B_3^\rho B_3^\lambda \rangle \propto \delta^{\rho\lambda}$.

D Evaluation of the static potential

In this appendix we explicitly show the intermediate steps which lead to the final expression of the static potentials in eq. (4.15) and (4.16).

D.1 Spin-independent contribution

Starting from eq. (4.10), the leading spin-independent static potential can be written as

$$\mathcal{U}_{\text{SI}_1}(\mathbf{r}_1, \mathbf{r}_2; x_3) = -\frac{g_E^2}{N_c} \left\langle \text{Tr} \left\{ \left[\mathcal{A}^+(\mathbf{r}_1, x_3) + \mathcal{A}^-(\mathbf{r}_2, x_3) \right] \times \right. \right. \quad (\text{D.1})$$

$$\left. \left. \int_0^{x_3} dz_3 \left[\mathcal{A}^+\left(\frac{z_3}{x_3} \mathbf{r}_1, z_3\right) + \mathcal{A}^-\left(\frac{z_3}{x_3} \mathbf{r}_2, z_3\right) \right] \right\} \right\rangle = 2g_E^2 C_F \left[\mathcal{V}^-(\mathbf{r}_1, \mathbf{r}_2, x_3) - \mathcal{V}^+(\mathbf{r}_1, \mathbf{r}_1, x_3) \right].$$

where, we contracted the gauge fields and, similarly to the procedure used in Ref. [11], we introduced the integrals

$$\mathcal{V}^\pm(\mathbf{r}_1, \mathbf{r}_2, x_3) = -\int_0^{x_3} dz_3 \left[\Delta_{33} \left(\mathbf{r}_1 - \mathbf{r}_2 + \frac{z_3}{x_3} \mathbf{r}_2, z_3 \right) \mp \Delta_{00} \left(\mathbf{r}_1 - \mathbf{r}_2 \frac{z_3}{x_3} \mathbf{r}_2, z_3 \right) \right], \quad (\text{D.2})$$

where $\Delta_{\mu\nu}$ is the gauge field propagator defined in eq. (B.1), in which we made explicit the dependence on the transverse and longitudinal coordinates. Notice that it holds $\mathcal{V}^\pm(\mathbf{r}_1, \mathbf{r}_2, x_3) = \mathcal{V}^\pm(\mathbf{r}_2, \mathbf{r}_1, x_3)$ under the exchanges $\mathbf{r}_1 \leftrightarrow \mathbf{r}_2$. By taking the large separation limit in the third spatial direction, see eq. (C.7) and (C.9) of Ref. [11], we arrive at

$$U_{\text{SI}_1}(\mathbf{r}_1 - \mathbf{r}_2) = \lim_{x_3 \rightarrow \infty} \mathcal{U}_{\text{SI}_1}(\mathbf{r}_1, \mathbf{r}_2, x_3) = \frac{g_E^2 C_F}{2\pi} \left[\ln \left(\frac{m_E r}{2} \right) + \gamma_E - K_0(m_E r) \right], \quad (\text{D.3})$$

where we introduced $r = |\mathbf{r}_1 - \mathbf{r}_2|$, γ_E is the Euler-Mascheroni constant, K_0 is a modified Bessel function, and m_E is the Debye mass introduced in eq. (3.2). The potential above is exactly the expression reported in (4.15), and which was found in Ref. [10].

D.2 Spin-dependent contribution

Analogously, the temperature-suppressed, spin-dependent potential in eq. (4.12) can be written as

$$\mathcal{U}_{\mathcal{O}}(\mathbf{r}_1, \mathbf{r}_2, x_3) = -g_E^2 \frac{2s_{\mathcal{O}} C_F}{(2\pi T)^2} \mathcal{B}(\mathbf{r}_1, \mathbf{r}_2, x_3), \quad (\text{D.4})$$

where we introduced the definition

$$\mathcal{B}(\mathbf{r}_1, \mathbf{r}_2, x_3) = \frac{1}{N_c^2 - 1} \int_0^{x_3} dz_3 \left\langle \text{Tr} \left\{ B_3(\mathbf{r}_1, x_3) B_3\left(\frac{z_3}{x_3} \mathbf{r}_2, z_3\right) + B_3(\mathbf{r}_2, x_3) B_3\left(\frac{z_3}{x_3} \mathbf{r}_1, z_3\right) \right\} \right\rangle. \quad (\text{D.5})$$

By taking the contractions of the gauge fields in eq. (B.1), and by expressing the chromomagnetic field as in eq. (A.4), the integral can be written as⁵

$$\begin{aligned} B(\mathbf{r}_1 - \mathbf{r}_2) &= \lim_{x_3 \rightarrow \infty} \mathcal{B}(\mathbf{r}_1, \mathbf{r}_2, x_3) \\ &= \lim_{x_3 \rightarrow \infty} \int_0^{x_3} dz_3 \left[\partial_1^{\mathbf{r}_2} \partial_1^{\mathbf{r}_1} \Delta_{22}(\mathbf{r}_1 - \mathbf{r}_2, x_3 - z_3) + \partial_2^{\mathbf{r}_2} \partial_2^{\mathbf{r}_1} \Delta_{11}(\mathbf{r}_1 - \mathbf{r}_2, x_3 - z_3) \right]. \end{aligned} \quad (\text{D.6})$$

⁵Here the superscript in the partial derivative refers to which \mathbf{r}_i (either \mathbf{r}_1 or \mathbf{r}_2) the derivative is taken with respect to. Therefore $\partial_i^{\mathbf{r}_j}$ indicates the partial derivative with respect to the i th component of the \mathbf{r}_j coordinate.

By recalling the expression of the spatial components of the gluon propagators, see eq. (B.2), the derivative terms in the expression above read

$$\partial_j^{\mathbf{r}_2} \partial_j^{\mathbf{r}_1} \Delta_{ii}(\mathbf{r}_1 - \mathbf{r}_2, x_3 - z_3) = \int \frac{d^3 p}{(2\pi)^3} e^{i\mathbf{p}(\mathbf{r}_1 - \mathbf{r}_2)} e^{ip_3(x_3 - z_3)} \frac{p_j^2}{p^2}. \quad (\text{D.7})$$

By inserting this expression in eq. (D.6), the integral can be written as

$$B(\mathbf{r}_1 - \mathbf{r}_2) = \lim_{x_3 \rightarrow \infty} \int_0^{x_3} dz_3 \int \frac{d^3 p}{(2\pi)^3} e^{i\mathbf{p}(\mathbf{r}_1 - \mathbf{r}_2)} e^{ip_3(x_3 - z_3)} \left[1 - \frac{p_3^2}{p^2} \right], \quad (\text{D.8})$$

where we used the fact that $p^2 - p_3^2 = p_1^2 + p_2^2 = \mathbf{p}^2$. Therefore the integral above can be split into two different contributions as

$$\begin{aligned} B(\mathbf{r}_1 - \mathbf{r}_2) &= \lim_{x_3 \rightarrow \infty} \left[\delta^{(2)}(\mathbf{r}_1 - \mathbf{r}_2) \int_0^{x_3} dz_3 \delta(x_3 - z_3) - \mathcal{R}(\mathbf{r}_1 - \mathbf{r}_2, x_3) \right] \\ &= \frac{1}{2} \delta^{(2)}(\mathbf{r}_1 - \mathbf{r}_2) - \lim_{x_3 \rightarrow \infty} \mathcal{R}(\mathbf{r}_1 - \mathbf{r}_2, x_3), \end{aligned} \quad (\text{D.9})$$

where we have introduced the remainder time-integral

$$\mathcal{R}(\mathbf{r}_1 - \mathbf{r}_2, x_3) = \int \frac{dp_3}{2\pi} p_3^2 \int_0^{x_3} dz_3 e^{ip_3(x_3 - z_3)} \int \frac{d^2 \mathbf{p}}{(2\pi)^2} \frac{e^{i\mathbf{p}(\mathbf{r}_1 - \mathbf{r}_2)}}{\mathbf{p}^2 + p_3^2}. \quad (\text{D.10})$$

The integration over the transverse components of the momentum can be carried out by recalling that it holds

$$\int \frac{d^2 \mathbf{p}}{(2\pi)^2} \frac{e^{i\mathbf{p}(\mathbf{r}_1 - \mathbf{r}_2)}}{\mathbf{p}^2 + p_3^2} = \frac{1}{2\pi} K_0(|p_3| r), \quad (\text{D.11})$$

where K_0 is a modified Bessel function. Analogously by performing the integration over the longitudinal spatial coordinate, the integral in eq. (D.10) is reduced to a one-dimensional integral over the p_3 variable that reads

$$\mathcal{R}(\mathbf{r}_1 - \mathbf{r}_2, x_3) = \frac{i}{2\pi} \int \frac{dp_3}{2\pi} p_3 (1 - e^{ip_3 x_3}) K_0(|p_3| r). \quad (\text{D.12})$$

Finally the integral over the longitudinal momentum can be carried out by taking into account the symmetry properties of the integrand under the change $p_3 \rightarrow -p_3$, yielding to

$$\mathcal{R}(\mathbf{r}_1 - \mathbf{r}_2, x_3) = \frac{1}{2\pi^2} \int_0^\infty dp_3 p_3 \sin(p_3 x_3) K_0(p_3 r) = \frac{x_3}{4\pi (x_3^2 + r^2)^{3/2}}. \quad (\text{D.13})$$

Therefore by taking the large separation limit in the third spatial direction in eq. (D.6), and by recalling that, according to eq. (D.13), $\lim_{x_3 \rightarrow \infty} \mathcal{R}(\mathbf{r}_1 - \mathbf{r}_2, x_3) = 0$, we obtain

$$B(\mathbf{r}_1 - \mathbf{r}_2) = \frac{1}{2} \delta^{(2)}(\mathbf{r}_1 - \mathbf{r}_2). \quad (\text{D.14})$$

Finally, by inserting this expression into eq. (D.4) we obtain the final expression for the spin-dependent static potential

$$U_{\mathcal{O}}(\mathbf{r}_1 - \mathbf{r}_2) = \lim_{x_3 \rightarrow \infty} \mathcal{U}_{\mathcal{O}}(\mathbf{r}_1, \mathbf{r}_2, x_3) = -g_E^2 \frac{s_{\mathcal{O}} C_F}{(2\pi T)^2} \delta^{(2)}(\mathbf{r}_1 - \mathbf{r}_2) \quad (\text{D.15})$$

reported in eq. (4.16).

References

- [1] A.D. Linde, *Infrared problem in thermodynamics of the Yang-Mills gas*, *Phys. Lett. B* **96** (1980) 289.
- [2] E. Braaten and A. Nieto, *Free energy of QCD at high temperature*, *Phys. Rev. D* **53** (1996) 3421 [[hep-ph/9510408](#)].
- [3] K. Kajantie, M. Laine, K. Rummukainen and Y. Schröder, *Pressure of hot QCD up to $g^6 \ln(1/g)$* , *Phys. Rev. D* **67** (2003) 105008 [[hep-ph/0211321](#)].
- [4] S. Borsanyi, G. Endrodi, Z. Fodor, S. Katz and K. Szabo, *Precision $SU(3)$ lattice thermodynamics for a large temperature range*, *JHEP* **1207** (2012) 056 [[1204.6184](#)].
- [5] L. Giusti and M. Pepe, *Equation of state of the $SU(3)$ Yang–Mills theory: A precise determination from a moving frame*, *Phys. Lett. B* **769** (2017) 385 [[1612.00265](#)].
- [6] M. Dalla Brida, L. Giusti and M. Pepe, *Non-perturbative definition of the QCD energy-momentum tensor on the lattice*, *JHEP* **04** (2020) 043 [[2002.06897](#)].
- [7] M. Dalla Brida, L. Giusti, T. Harris, D. Laudicina and M. Pepe, *Non-perturbative thermal QCD at all temperatures: the case of mesonic screening masses*, *JHEP* **04** (2022) 034 [[2112.05427](#)].
- [8] L. Giusti, T. Harris, D. Laudicina, M. Pepe and P. Rescigno, *Baryonic screening masses in QCD at high temperature*, *Phys. Lett. B* **855** (2024) 138799 [[2405.04182](#)].
- [9] M. Bresciani, M.D. Brida, L. Giusti and M. Pepe, *The QCD Equation of State with $N_f = 3$ flavours up to the electro-weak scale*, [2501.11603](#).
- [10] M. Laine and M. Vepsalainen, *Mesonic correlation lengths in high temperature QCD*, *JHEP* **02** (2004) 004 [[hep-ph/0311268](#)].
- [11] L. Giusti, M. Laine, D. Laudicina, M. Pepe and P. Rescigno, *Baryonic thermal screening mass at NLO*, *JHEP* **06** (2024) 205 [[2405.03975](#)].
- [12] A. Bazavov et al., *Meson screening masses in $(2+1)$ -flavor QCD*, *Phys. Rev. D* **100** (2019) 094510 [[1908.09552](#)].
- [13] N. Brambilla et al., *Heavy Quarkonium: Progress, Puzzles, and Opportunities*, *Eur. Phys. J. C* **71** (2011) 1534 [[1010.5827](#)].
- [14] T.H. Hansson and I. Zahed, *Hadronic correlators in hot QCD*, *Nucl. Phys. B* **374** (1992) 277.
- [15] P.H. Ginsparg, *First and second order phase transitions in gauge theories at finite temperature*, *Nucl. Phys. B* **170** (1980) 388.
- [16] T. Appelquist and R.D. Pisarski, *High-temperature Yang-Mills theories and three-dimensional Quantum Chromodynamics*, *Phys. Rev. D* **23** (1981) 2305.

- [17] M. Laine and A. Vuorinen, *Basics of Thermal Field Theory*, vol. 925, Springer Lecture Notes in Physics (2016), [10.1007/978-3-319-31933-9](https://doi.org/10.1007/978-3-319-31933-9), [[1701.01554](https://arxiv.org/abs/1701.01554)].
- [18] J.I. Kapusta, *Quantum Chromodynamics at high temperature*, *Nucl. Phys. B* **148** (1979) 461.
- [19] M. Laine and Y. Schroder, *Two-loop QCD gauge coupling at high temperatures*, *JHEP* **03** (2005) 067 [[hep-ph/0503061](https://arxiv.org/abs/hep-ph/0503061)].
- [20] I. Ghisoiu, J. Möller and Y. Schröder, *Debye screening mass of hot Yang-Mills theory to three-loop order*, *JHEP* **11** (2015) 121 [[1509.08727](https://arxiv.org/abs/1509.08727)].
- [21] S.-z. Huang and M. Lissia, *The dimensionally reduced effective theory for quarks in high-temperature QCD*, *Nucl. Phys. B* **480** (1996) 623 [[hep-ph/9511383](https://arxiv.org/abs/hep-ph/9511383)].
- [22] W.E. Caswell and G.P. Lepage, *Effective Lagrangians for bound state problems in QED, QCD, and other field theories*, *Phys. Lett. B* **167** (1986) 437.
- [23] N. Brambilla, A. Pineda, J. Soto and A. Vairo, *Potential NRQCD: an effective theory for heavy quarkonium*, *Nucl. Phys. B* **566** (2000) 275 [[hep-ph/9907240](https://arxiv.org/abs/hep-ph/9907240)].
- [24] B.B. Brandt, A. Francis, M. Laine and H.B. Meyer, *A relation between screening masses and real-time rates*, *JHEP* **05** (2014) 117 [[1404.2404](https://arxiv.org/abs/1404.2404)].
- [25] D. Bala, O. Kaczmarek, P. Petreczky, S. Sharma and S. Tah, *The spatial string tension and its effects on screening correlators in a thermal QCD plasma*, [2501.17943](https://arxiv.org/abs/2501.17943).